

See discussions, stats, and author profiles for this publication at: <https://www.researchgate.net/publication/254883323>

# Native Defects and the Dehydrogenation of $\text{NaBH}_4$

ARTICLE *in* THE JOURNAL OF PHYSICAL CHEMISTRY C · DECEMBER 2011

Impact Factor: 4.77 · DOI: 10.1021/jp208642g

---

CITATIONS

6

---

READS

11

3 AUTHORS, INCLUDING:



Deniz Çakır

University of Antwerp

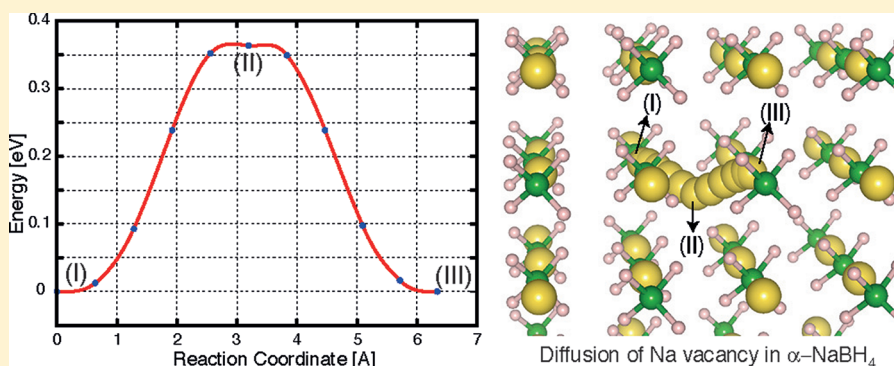
33 PUBLICATIONS 263 CITATIONS

SEE PROFILE

Native Defects and the Dehydrogenation of NaBH<sub>4</sub>Deniz Çakır,<sup>†</sup> Gilles A. de Wijs,<sup>‡</sup> and Geert Brocks<sup>\*,†</sup><sup>†</sup>Computational Materials Science, Faculty of Science and Technology and MESA+ Institute for Nanotechnology, University of Twente, P.O. Box 217, 7500 AE Enschede, The Netherlands<sup>‡</sup>Radboud University Nijmegen, Institute for Molecules and Materials, Heyendaalseweg 135, 6525 AJ Nijmegen, The Netherlands

S Supporting Information

## ABSTRACT:



Chemical reactions of hydrogen storage materials often involve mass transport through a bulk solid. Diffusion in crystalline solids proceeds by means of lattice defects. Using density functional theory (DFT) calculations, we identify the stability and the mobility of the most prominent lattice defects in the hydrogen storage material NaBH<sub>4</sub>. At experimental dehydrogenation conditions, the Schottky defects of missing Na<sup>+</sup> and BH<sub>4</sub><sup>−</sup> ions form the main vehicle for mass transport in NaBH<sub>4</sub>. Substituting a BH<sub>4</sub><sup>−</sup> by a H<sup>−</sup> ion yields the most stable defect, locally converting NaBH<sub>4</sub> into NaH. Such a substitution most likely occurs at the surface of NaBH<sub>4</sub>, releasing BH<sub>3</sub>. Adding Mg or MgH<sub>2</sub> to NaBH<sub>4</sub> promotes this scenario.

## 1. INTRODUCTION

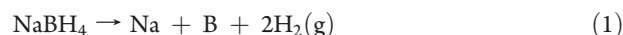
The interest in lightweight metal borohydrides as hydrogen storage materials is triggered by their exceptionally high gravimetric hydrogen density. Borohydrides have been studied intensively in recent years, both experimentally<sup>1,2</sup> and by density functional theory (DFT) calculations.<sup>3–6</sup> Although borohydrides are reactive materials, they are fairly stable with respect to decomposition and release hydrogen at temperatures that are too high for practical applications. Moreover, the kinetics of hydrogen desorption and adsorption is slow, and the reactions are often found to be irreversible under practical conditions.

The relative stability of borohydrides can be modified by mixing them with simple hydrides such as MgH<sub>2</sub> or amides such as LiNH<sub>2</sub>. These so-called reactive composites yield dehydrogenation products that are more stable than those of the pure borohydrides, which decreases the borohydride's relative stability.<sup>7</sup> The (de)hydrogenation kinetics of reactive composites is often better than that of pure borohydrides<sup>8</sup> but still not sufficiently fast. Insight in the bottlenecks of the reaction kinetics can help to give directions on how to improve the kinetics or identify fundamental barriers.

As most of the components involved in the (de)hydrogenation reactions are solid crystalline materials, and the reaction products are separated on a macroscopic scale, mass transport

has to take place through solid bulk materials. Mass transport inside a crystal proceeds by means of lattice defects. To understand such transport in hydrogen storage materials, one therefore has to study the relative abundance and the mobility of intrinsic defects.

Here we focus on NaBH<sub>4</sub>, which is a well-known material that desorbs hydrogen according to the reaction<sup>9,10</sup>



Alternatively, decomposition might occur according to the reaction  $\text{NaBH}_4 \rightarrow \text{NaH} + \text{B} + (3/2)\text{H}_2$ . However, substantial dehydrogenation of NaBH<sub>4</sub> (i.e., giving hydrogen gas pressures ~1 bar) is observed in experiment only at temperatures where decomposition of NaBH<sub>4</sub> directly to the elements is favored, as in reaction 1.<sup>9,10</sup> Alternative reaction products such as NaB<sub>12</sub>H<sub>12</sub>, which do not seem to be prominent in these reactions,<sup>11</sup> are not considered in this paper.

The reactive composite NaBH<sub>4</sub>/MgH<sub>2</sub> has served as a model system to study reaction mechanisms and kinetics in borohydride composites.<sup>12–14</sup> One reason for choosing this as a model system

Received: September 7, 2011

Revised: October 27, 2011

Published: October 27, 2011

is provided by the relatively simple crystal structures of the compounds involved, which facilitates monitoring the reactions by X-ray diffraction, for instance. The structure of NaBH<sub>4</sub> is NaCl-like with BH<sub>4</sub><sup>−</sup> ions replacing Cl<sup>−</sup>. Mixing NaBH<sub>4</sub> with MgH<sub>2</sub> would ideally lead to the reaction 2NaBH<sub>4</sub> + MgH<sub>2</sub> → 2NaH + MgB<sub>2</sub> + 4H<sub>2</sub>(g). However, similar to the pure NaBH<sub>4</sub> case, substantial dehydrogenation of the NaBH<sub>4</sub>/MgH<sub>2</sub> composite only occurs at high temperatures, where the simple metal hydrides are unstable. Upon heating the composite, first dehydrogenation of MgH<sub>2</sub> to Mg proceeds at  $T \approx 600$  K, followed by dehydrogenation of NaBH<sub>4</sub> at  $T \approx 700$  K, forming MgB<sub>2</sub> and Na.<sup>12,13</sup> The relevant reaction therefore is



In this paper, we identify the type, the stability, and the mobility of lattice defects in NaBH<sub>4</sub> by means of first-principles DFT calculations. In previous calculations it has been argued that H-related interstitials are the dominant defects responsible for mass transport, in particular the neutral interstitial H<sub>2</sub> molecule.<sup>15</sup> We find that this is true only under very H-rich conditions, i.e., at a very low temperature or at a very high hydrogen gas pressure. Instead, at the experimental conditions corresponding to the reactions given by eq 1 and eq 2, the charged defects of missing Na<sup>+</sup> or BH<sub>4</sub><sup>−</sup> ions are prominent. As they determine the charge balance in NaBH<sub>4</sub>, they occur in stoichiometric units. The barriers for diffusion of these vacancies are quite low, so these defects form the main vehicle for mass transport through the lattice. This is vital to separate B and Na on a macroscopic scale, as required by the reactions (eq 1 and eq 2).

Substituting a BH<sub>4</sub><sup>−</sup> ion by a H<sup>−</sup> ion yields the most stable defect, whereby NaBH<sub>4</sub> is locally converted into NaH.<sup>14</sup> Of the neutral impurities, a H divacancy is reasonably stable. However, this defect is immobile, and as it binds two B atoms, it blocks mass transport of B. In eq 2, the H divacancy is relatively less abundant than in the simple reaction (eq 1), which could explain the faster kinetics of the composite reaction. Interstitials, whether H-related, Na-related, or molecules such as BH<sub>3</sub>, are unstable under experimental conditions.

All information combined suggests a scenario where BH<sub>4</sub><sup>−</sup> ions decompose at the surface of NaBH<sub>4</sub> into H<sup>−</sup> ions and BH<sub>3</sub> molecules. The H<sup>−</sup> ions stay in the lattice, locally converting NaBH<sub>4</sub> into NaH. The BH<sub>3</sub> molecules can enter the gas phase or immediately react to form the products of the reactions (eq 1 and eq 2).

## 2. COMPUTATIONAL METHODS

In calculating the formation energy  $E_f[X^q]$  of a defect of type  $X$  and charge  $q$ , we follow the procedure outlined by van de Walle and co-workers.<sup>16</sup>

$$E_f[X^q] = E_{\text{tot}}[X^q] - E_{\text{bulk}} + qE_F - \sum_i n_i \mu_i \quad (3)$$

where  $E_{\text{tot}}[X^q]$  and  $E_{\text{bulk}}$  are the total energies of a supercell with and without the defect, respectively. We include zero point vibration energies (ZPEs) in these total energies, as their contribution is not negligible. To charge a defect, electrons are added at or taken from the Fermi level  $E_F$ . Of course, for each supercell the Fermi energy has to be taken with respect to the same reference potential. We have used the electrostatic potential on a Na atom far removed from the defect as reference potential. In the absence of significant extrinsic doping, the Fermi

level is fixed by charge neutrality; i.e., the concentration of negatively and positively charged intrinsic defects must be equal. We determine the Fermi level by demanding overall charge neutrality.

All  $n_i$  atoms of species  $i$  comprising a specific defect are taken from reservoirs at chemical potentials  $\mu_i$ . The latter are fixed by the experimental conditions, specifically by the Gibbs free energies of the phases in equilibrium.<sup>16,17</sup> We neglect  $T$  and  $P$  effects, including heats of fusion, on the chemical potentials of solids, as these effects are relatively small.<sup>18–20</sup> This implies that for the solid phases we use total energies at  $T = 0$  instead of free energies.

In contrast, the chemical potential of a gas is strongly  $T$  and  $P$  dependent. For hydrogen, we use  $\mu_{\text{H}} = (1/2)E_{\text{tot}}(\text{H}_2) + \Delta\mu_{\text{H}}$ , with  $E_{\text{tot}}(\text{H}_2)$  being the DFT+ZPE total energy of a H<sub>2</sub> molecule and

$$\Delta\mu_{\text{H}} = \frac{1}{2} \left[ \Delta G_0(T) + k_{\text{B}} T \ln \frac{P_{\text{H}_2}}{P_0} \right] \quad (4)$$

$\Delta G_0(T)$  is the change in Gibbs free energy per H<sub>2</sub> molecule in a gas at temperature  $T$  and pressure  $P_0 = 1$  bar, with  $\Delta G_0(0) = 0$ . Note that  $\Delta G_0(T)$  decreases monotonically with increasing  $T$  and that it is large under typical experimental conditions, e.g.,  $\Delta G_0(700 \text{ K}) = -0.92 \text{ eV}$ .<sup>21,22</sup> The last term in eq 4 models the pressure dependence according to the ideal gas law.

Within the transition state model, the defect's mobility is determined by the frequency of jumps between neighboring minimum energy sites

$$\nu[X^q] = \nu_0[X^q] \exp \left[ -\frac{E_{\text{m}}[X^q]}{k_{\text{B}} T} \right] \quad (5)$$

with  $E_{\text{m}}[X^q]$  being the migration barrier and  $\nu_0[X^q]$  the attempt frequency. The latter typically has a value  $\sim 10^{12} - 10^{13} \text{ Hz}$  and usually does not depend very critically on the type of defect. In contrast, different values of  $E_{\text{m}}[X^q]$  for different defects easily result in  $\nu[X^q]$  varying by several orders of magnitude. In this paper, we therefore concentrate on calculating  $E_{\text{m}}[X^q]$ . Often the equilibrium concentration of a defect is too small to give rise to significant mass transport. The latter then proceeds through so-called self-diffusion, where a defect first has to be created before it migrates. The activation energy for self-diffusion is given by

$$E_{\text{a}}[X^q] = E_{\text{f}}[X^q] + E_{\text{m}}[X^q] \quad (6)$$

The diffusivity of a defect can be obtained via the usual relation  $D = Na^2\nu[X^q]/6$ , with  $N$  being the number of neighboring minimum energy sites and  $a$  the distance to such a site.

Total energies are calculated using the Vienna Ab initio Simulation Package (VASP) with Projector Augmented Waves (PAWs) and the PW91 generalized gradient approximation (GGA) functional.<sup>23–26</sup> We use a plane wave kinetic energy cutoff of 400 eV and a regular  $k$ -point grid with a spacing of  $0.02 \text{ \AA}^{-1}$  for the Brillouin zone sampling. Total energies are then converged to within 0.02 eV/formula unit. The total energy of a defect is calculated using a NaBH<sub>4</sub>  $2 \times 2 \times 2$  cubic supercell with a lattice parameter of 12.22 Å, containing 192 atoms. The convergence has been checked by varying the size of the supercell. Calculations with a  $3 \times 3 \times 3$  supercell, containing 648 atoms, show that total energies of charged and neutral defects are then converged on a scale of 0.1 and 0.01 eV, respectively. Migration barriers are calculated with the climbing image nudged elastic band method.<sup>27</sup>

**Table 1.** Calculated  $\Delta$ ZPEs (eV) of Defects  $X^q$ 

$X^q$	$\Delta$ ZPE	$X^q$	$\Delta$ ZPE	$X^q$	$\Delta$ ZPE
$V_{\text{BH}_4}^+$	−0.34	$V_{2\text{H}}^0$	−0.13	$\text{BH}_{3,i}$	0.47
$V_{\text{BH}_3}^0$	−0.36	$V_{\text{H}}^-$	−0.10	$\text{H}_i^-$	−0.01
		$V_{\text{H}}^+$	0.03	$\text{H}_i^+$	0.16

ZPEs are constructed from the phonon frequencies calculated by diagonalizing the dynamical matrix of force constants. The latter are obtained as central differences from the forces on all atoms after displacing each atom, one at a time, by  $\pm 0.01$  Å. The high frequency modes in alkali borohydrides, which comprise most of the ZPEs, are the internal vibrations of the  $\text{BH}_4$  units.<sup>3,28,29</sup> It is therefore not surprising to find that the most prominent ZPE contributions to the total energy of a defect come from the  $\text{BH}_4$  units that are directly affected by the defect. For instance, only a single  $\text{BH}_4$  unit is changed in the case of a H-related point defect and only two  $\text{BH}_4$  units in the case of a H-divacancy. The high frequency motions of all other  $\text{BH}_4$  units are then hardly affected by the defect. In calculating ZPEs, one can consider the internal vibrations of one or two  $\text{BH}_4$  units only, which brings down the cost of calculating ZPE contributions considerably.

For a single  $\text{BH}_4$  unit in  $\text{NaBH}_4$ , we find  $\text{ZPE} = 1.024$  eV, which is in good agreement with the value of 0.989 eV extracted from the experimental spectra.<sup>3</sup> For the ZPE of  $\text{H}_2$  and B, we use the values obtained in previous calculations.<sup>18,19</sup> The ZPEs of Na and Mg are negligible.<sup>30,31</sup> Table 1 gives the  $\Delta$ ZPE associated with the formation of a number of prominent H-related defects. As H-atoms bonded in a  $\text{BH}_4$  unit are more confined than in a  $\text{H}_2$  molecule, the  $\Delta$ ZPE of H-related vacancies tends to be negative, whereas that of H-related interstitials tends to be positive. Table 1 shows that the ZPE contribution to the defect formation energy in borohydrides is neither necessarily negligible nor “symmetric”, as it favors vacancies over interstitials. The ZPE contributions for  $\text{BH}_x$ -type defects are particularly large.

### 3. RESULTS

The hydrogen chemical potential can be fixed according to eq 4. We choose a temperature  $T = 700$  K, which is in the typical range of the experiments, for both eq 1 and eq 2.<sup>9,10,12–14</sup> Choosing a  $\text{H}_2$  gas pressure  $P_{\text{H}_2} = 1$  bar then gives  $\Delta\mu_{\text{H}} = \mu_{\text{H}} - \mu_{\text{H}}(T = 0) = -0.46$  eV.<sup>21,22</sup>

As discussed in the previous section, we approximate the Gibbs free energies of solids by ( $T = 0$ ) total energies. For eq 1, this leads to chemical potentials  $\mu_{\text{B}} = E_{\text{tot}}(\text{B})$  and  $\mu_{\text{Na}} = E_{\text{tot}}(\text{Na})$ , the DFT total energies per atom of bulk  $\alpha$ -B, and the bulk Na metal, respectively. To check whether the hydrogen chemical potential given above is a sensible choice for our calculations, we can use the relation  $\mu_{\text{Na}} + \mu_{\text{B}} + 4\mu_{\text{H}} = E_{\text{tot}}(\text{NaBH}_4)$ . This relation assumes equilibrium between the phases involved in eq 1, with  $E_{\text{tot}}(\text{NaBH}_4)$  being the total energy of bulk  $\text{NaBH}_4$  approximating the corresponding free energy.<sup>16,17</sup> We use the cubic  $\alpha$ - $\text{NaBH}_4$  structure in this calculation, as well as in all subsequent calculations.<sup>10,32</sup> From this calculation, we find  $\Delta\mu_{\text{H}} = -0.42$  eV for the reaction (eq 1) equilibrium, which is close to the value  $-0.46$  eV given above. Such a good agreement might be a bit fortuitous in view of the accuracy of DFT and the approximations we made. Moreover, nonequilibrium conditions may be applicable, as borohydride materials exhibit kinetic (de)hydrogenation

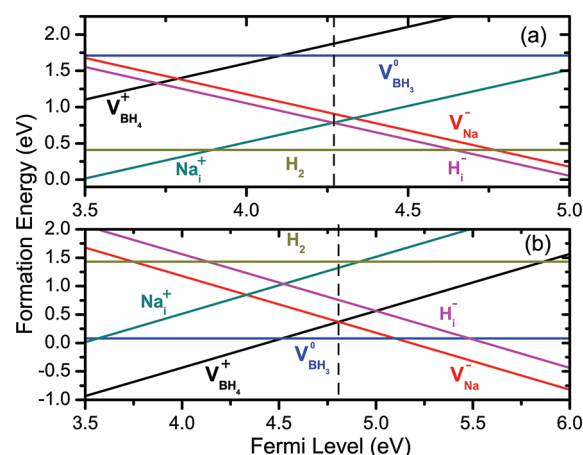


**Figure 1.** Formation energy  $E_{\text{f}}[X^q]$  of intrinsic defects as a function of the Fermi level  $E_{\text{F}}$  under (a) H-rich conditions ( $T = 0$ ) and (b) under conditions corresponding to eq 1 ( $T = 700$  K,  $P_{\text{H}_2} = 1$  bar). The vertical lines denote  $E_{\text{F}}$  determined by overall charge neutrality on the basis of charged intrinsic defects.

**Table 2.** Formation Energies  $E_{\text{f}}[X^q]$  (eV) of Defects  $X^q$  at H-Rich ( $T = 0$  K) Conditions and at H-Poor ( $T = 700$  K and  $P_{\text{H}_2} = 1$  bar) Conditions for Equation 1 and Equation 2

$X^q$	$T = 0^a$	eq 1 <sup>b</sup>	eq 2 <sup>c</sup>	$X^q$	$T = 0^a$	eq 1 <sup>b</sup>	eq 2 <sup>c</sup>
$V_{\text{BH}_4}^+$	1.87	0.37	0.26	$\text{Na}_i^+$	0.78	1.32	1.44
$V_{\text{Na}}^+$	0.91	0.37	0.26	$\text{BH}_{3,i}^0$	0.95	2.48	2.70
$V_{\text{BH}_3}^0$	1.71	0.08	−0.14	$\text{H}_{2,i}^0$	0.41	1.43	1.43
$V_{2\text{H}}^0$	1.54	0.52	0.52	$\text{H}_i^-$	0.78	0.76	0.64
$V_{\text{H}}^-$	1.83	0.78	0.67	$\text{H}_i^+$	2.59	3.63	3.75
$V_{\text{H}}^+$	2.25	2.28	2.39				

<sup>a</sup>  $\Delta\mu_{\text{H}} = 0$ ,  $\Delta\mu_{\text{B}} = 0$ . <sup>b</sup>  $\Delta\mu_{\text{H}} = -0.46$  eV,  $\Delta\mu_{\text{B}} = 0$ . <sup>c</sup>  $\Delta\mu_{\text{H}} = -0.46$  eV,  $\Delta\mu_{\text{B}} = -0.24$  eV.

bottlenecks experimentally. In the following, we use  $\Delta\mu_{\text{H}} = -0.46$  when referring to eq 1, as well as to eq 2, in this paper.

In discussing the defect formation energies related to eq 2, we keep  $\mu_{\text{Na}} = E_{\text{tot}}(\text{Na})$  and set  $\mu_{\text{Mg}} = E_{\text{tot}}(\text{Mg})$ , the total energy of bulk metal Mg. Assuming equilibrium between the  $\text{MgB}_2$  and Mg phases, then fixes  $\mu_{\text{B}}$  by

$$\mu_{\text{Mg}} + 2\mu_{\text{B}} = E_{\text{tot}}(\text{MgB}_2) \quad (7)$$

with  $E_{\text{tot}}(\text{MgB}_2)$  being the DFT total energy per formula unit of bulk  $\text{MgB}_2$ . Equation 7 leads to a value of  $\mu_{\text{B}}$  that is 0.24 eV lower than the value extracted from bulk  $\alpha$ -B. We refer to this value as  $\Delta\mu_{\text{B}} = -0.24$  eV. One may expect that a decrease of the B chemical potential leads to a decrease of the formation energies of B-related vacancies in  $\text{NaBH}_4$  (cf. eq 3).

In a number of previous DFT calculations involving  $\text{NaBH}_4$ , a hydrogen chemical potential corresponding to  $\Delta\mu_{\text{H}} = 0$  has been used.<sup>13,33</sup> This then corresponds to H-rich conditions, i.e., low temperature,  $T \approx 0$  K, or high pressure, e.g.  $P_{\text{H}_2} = 5 \times 10^3$  bar at  $T = 700$  K (see eq 4), which are far from the usual experimental dehydrogenation conditions.

The formation energies of some prominent defects, calculated with chemical potentials for H-rich conditions ( $T = 0$ ) and for conditions corresponding to eq 1 ( $T = 700$  K,  $P_{\text{H}_2} = 1$  bar), are given in Figure 1 as a function of the Fermi level. At  $T = 0$  K the



interstitials  $\text{H}_i^-$  and  $\text{Na}_i^+$  are the charged defects with the lowest formation energies. The balance between these impurities determines charge neutrality and fixes the Fermi level at  $E_F = 4.27$  eV (with respect to the top of the valence band). The formation energies calculated at this Fermi level are given in Table 2.

H-rich conditions are reflected by the ease with which H-related interstitials are formed in the  $\text{NaBH}_4$  lattice. In particular, the neutral  $\text{H}_2$  molecule interstitial has the lowest formation energy of all defects listed in Table 2, in agreement with previous calculations.<sup>15</sup> Under such conditions, H-related vacancies, including  $\text{BH}_x$  vacancies, have a very high formation energy.

However, the experimental conditions at which dehydrogenation proceeds according to eq 1 and eq 2 are anything but H-rich. This is demonstrated by Figure 1(b). The charged defects with the smallest formation energies are now the vacancies  $\text{V}_{\text{BH}_4}^+$  and  $\text{V}_{\text{Na}}^-$ , which correspond to missing  $\text{BH}_4^-$  and  $\text{Na}^+$  ions in the lattice, respectively. Charge neutrality demands that the concentrations, and hence the formation energies, of these two defects are equal. The vacancies ( $\text{V}_{\text{BH}_4}^+$ ,  $\text{V}_{\text{Na}}^-$ ) are thus formed in stoichiometric units.

Such so-called Schottky defects are often the dominant defects in simple ionic materials such as  $\text{NaCl}$  or  $\text{MgO}$ , implying that in this respect  $\text{NaBH}_4$  qualifies as a simple ionic material. The Fermi level is calculated at  $E_F = 4.81$  and  $4.92$  eV for eq 1 and eq 2, respectively, and the corresponding formation energies are given in Table 2. H-related interstitials, including the interstitial  $\text{H}_2$  molecule, have a high formation energy under these conditions, making it highly unlikely that they play a significant role. This is in contrast to the conclusions of ref 15, which are based on H-rich conditions. Instead of H-related interstitials, H-related vacancies have a low formation energy under experimental conditions,  $\text{BH}_x$ -related vacancies in particular.

The neutral vacancy  $\text{V}_{\text{BH}_3}^0$  has the lowest formation energy of all studied defects under experimental conditions.  $\text{V}_{\text{BH}_3}^0$  in fact corresponds to substituting a  $\text{BH}_4^-$  ion by a  $\text{H}^-$  ion, and its low formation energy indicates the ease of this substitution.<sup>34</sup> Its consequences will be discussed in the next section.

The formation energy of all interstitials is unfavorably high, whether of H- or Na-type, or interstitial molecules such as  $\text{BH}_3$ , compared to the formation energies of the vacancies discussed above. This means that interstitials do not play a substantial role in the mass transport in  $\text{NaBH}_4$  under typical experimental conditions. The same holds for H-related vacancies, which correspond to partially decomposed  $\text{BH}_4$  moieties in the lattice. This suggests that decomposition of these moieties inside the lattice is unlikely and that the decomposition reaction takes place at the surface of  $\text{NaBH}_4$ . Of the most abundant simple defects,  $\text{V}_{\text{BH}_4}^+$ ,  $\text{V}_{\text{Na}}^-$ , and  $\text{V}_{\text{BH}_3}^0$ , the charged vacancies are quite mobile, as we will discuss below. These are therefore the prime vehicle for mass transport in  $\text{NaBH}_4$ .

Besides the mentioned vacancies, the neutral H atom divacancy  $\text{V}_{2\text{H}}^0$  has a fairly low formation energy. Creating H vacancies on two neighboring  $\text{BH}_4^-$  sites leads to a rebonding of the two remaining  $\text{BH}_3^-$  moieties to a  $\text{B}_2\text{H}_6^{2-}$  ion with an ethane-like structure.<sup>15</sup> As this ion is immobile, it does not contribute to mass transport, and hence it hampers the kinetics of decomposition. The number of possible ways to form the  $\text{B}_2\text{H}_6^{2-}$  ion is six times larger than that of a lattice point defect. With the formation energies of Table 2, the concentration of  $\text{B}_2\text{H}_6^{2-}$  at  $T = 700$  K is then comparable to that of the  $\text{V}_{\text{BH}_4}^+$  and  $\text{V}_{\text{Na}}^-$  vacancies for eq 1.

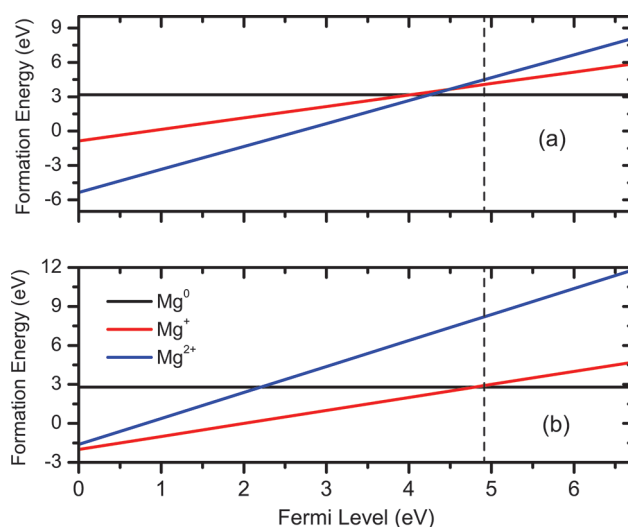


**Figure 2.** Formation energy (eV) of (a) interstitial and (b) substitutional Mg impurities as a function of the Fermi level. The intrinsic Fermi level at conditions corresponding to eq 2 lies at 4.92 eV.

Comparing the formation energies in the eq 1 and eq 2 columns in Table 2, one observes that in the latter the formation energies of  $\text{V}_{\text{BH}_4}^+$  and  $\text{V}_{\text{BH}_3}^0$  are lower. As expected, the participation of  $\text{Mg}/\text{MgB}_2$  phases in the reaction facilitates the formation of these boron-related vacancies in  $\text{NaBH}_4$ , as this involvement decreases the boron chemical potential. At the same time, the formation energy of  $\text{V}_{\text{Na}}^-$  decreases. This is because ( $\text{V}_{\text{BH}_4}^+$ ,  $\text{V}_{\text{Na}}^-$ ) pairs have to be formed in stoichiometric units because of charge neutrality. A lower  $\text{V}_{\text{BH}_4}^+$  formation energy then raises the Fermi level, which decreases the  $\text{V}_{\text{Na}}^-$  formation energy (see Figure 1).

In contrast, the formation energy of the H atom divacancy  $\text{V}_{2\text{H}}^0$  is not affected by the presence of  $\text{Mg}/\text{MgB}_2$ . The concentration of  $\text{B}_2\text{H}_6^{2-}$  at  $T = 700$  K is then roughly an order of magnitude smaller than that of  $\text{V}_{\text{BH}_4}^+$  and  $\text{V}_{\text{Na}}^-$  vacancies under conditions corresponding to eq 2. This is consistent with the faster kinetics of eq 2 compared to eq 1.

Besides by the presence of  $\text{Mg}/\text{MgB}_2$  phases, another possible way of influencing the defect balance would be to directly incorporate Mg impurities in the  $\text{NaBH}_4$  lattice. A low Mg impurity concentration does not change the Fermi level in  $\text{NaBH}_4$ . Interstitial Mg atoms are then preferably neutral (see Figure 2(a)), but have a very high formation energy of 3.17 eV. Mg atoms substituting Na atoms have a charge transition level  $\text{Mg}^+/\text{Mg}^{2+}$  that is very close to the intrinsic Fermi level (see Figure 2(b)). The formation energy of substitutional Mg is high, i.e., 2.75 eV. Increasing the Mg impurity concentration raises the Fermi level, which increases the formation energies even further, as shown by Figure 2. One can therefore conclude that the equilibrium concentration of Mg impurities in  $\text{NaBH}_4$  is negligible.

Having established the energetics of defects in the  $\text{NaBH}_4$  lattice, we investigate their mobility, where we restrict ourselves to the defects with the lowest formation energies, as these are the most relevant ones. The calculated migration barriers for the Schottky defects are  $E_m[\text{V}_{\text{BH}_4}^+] = 0.29$  eV and  $E_m[\text{V}_{\text{Na}}^-] = 0.37$  eV. The migration paths are quite simple, as illustrated in Figure 3. The vacancies migrate by interchanging with nearest neighbor ions in the lattice. Assuming an Arrhenius behavior, eq 5, with a typical attempt frequency  $\nu_0 = 10^{13}$  Hz, then leads to high

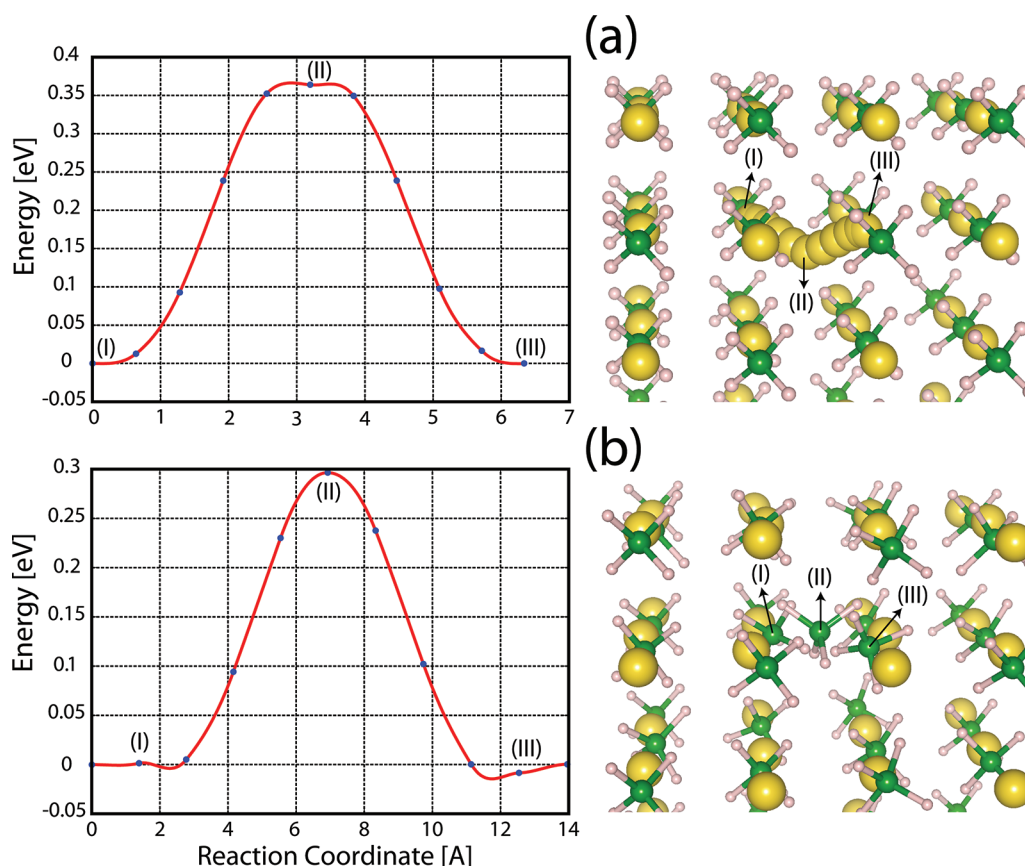


**Figure 3.** Diffusion of vacancies  $V_{\text{Na}}^-$  (a) and  $V_{\text{BH}_4}^+$  (b). Energies as a function of the reaction coordinate on the left-hand side. Diffusion paths on the right-hand side with begin, saddle, and end point configurations labeled by (I), (II), and (III), visualized using the VESTA program.<sup>35</sup>

hopping frequencies  $\nu$  for the vacancies in the range  $10^{10} - 10^{11}$  Hz at  $T = 700$  K.

The neutral vacancy  $V_{\text{BH}_3}^0$  corresponds to a  $\text{H}^-$  ion substituting a  $\text{BH}_4^-$  ion. To describe the migration of this defect one must therefore consider migration through the lattice of a substitutional  $\text{H}^-$  ion. This might proceed via a Frank–Turnbull mechanism, whereby the substitutional  $\text{H}^-$  first goes to an interstitial site, leaving behind a vacancy  $V_{\text{BH}_4}^+$ . The interstitial  $\text{H}^-$  then migrates through the lattice until it recombines with a vacancy  $V_{\text{BH}_4}^+$ . From the numbers given in Table 2, the activation energy of the first step is  $E_{\text{f}}[\text{H}_i^-] + E_{\text{f}}[V_{\text{BH}_4}^+] - E_{\text{f}}[V_{\text{BH}_3}^0] = 1.05$  eV under reaction (eq 1 and eq 2) conditions. This means that diffusion of this defect is much slower than that of the charged vacancies.

#### 4. DISCUSSION AND CONCLUSIONS

From the data assembled above, we propose a possible scenario for the decomposition of  $\text{NaBH}_4$ . The vacancies  $V_{\text{BH}_4}^+$  (missing  $\text{BH}_4^-$  ions) are the prime vehicles for transport of B and H in bulk  $\text{NaBH}_4$  and vacancies  $V_{\text{Na}}^-$  (missing  $\text{Na}^+$  ions) for transport of Na. At experimental conditions, the equilibrium concentration of these defects is still low, which means that transport is likely to proceed via self-diffusion, i.e., creation and subsequent diffusion. The activation energies for self-diffusion (eq 6) are  $E_{\text{a}}[V_{\text{BH}_4}^+] = 0.66$  eV and  $E_{\text{a}}[V_{\text{Na}}^-] = 0.74$  eV under conditions corresponding to eq 1. They decrease by 0.11 eV if the boron chemical potential is lowered through the participation of Mg/MgB<sub>2</sub> phases as in eq 2.

The vacancies ( $V_{\text{BH}_4}^+$ ,  $V_{\text{Na}}^-$ ) determine the charge balance at experimental conditions, which implies that the concentrations of these two vacancies are equal. Such Schottky defects, i.e., cation and anion vacancies formed in stoichiometric units, are among the most common defects in ionic materials. Alkali and alkaline earth borohydrides are ionic materials comprised of  $\text{BH}_4^-$  anions and  $\text{M}^+$  or  $\text{M}^{2+}$  cations. We suggest that Schottky defects, i.e.,  $\text{BH}_4^-$  and cation vacancies, are prominent defects in all alkali and alkaline earth borohydrides and responsible for mass transport. This agrees with the conclusion from NMR and Raman spectroscopy experiments on  $\text{LiBH}_4$  that H diffuses through the lattice in the form of  $\text{BH}_4$  units.<sup>29,36,37</sup>

$\text{BH}_4^-$  ions in the  $\text{NaBH}_4$  lattice are easily substituted by  $\text{H}^-$  ions, formally creating  $V_{\text{BH}_3}^0$  vacancies. Such a defect can be created by decomposing a  $\text{BH}_4^-$  ion into a  $\text{BH}_3$  molecule and a  $\text{H}^-$  ion.  $\text{BH}_3$  molecules are however not easily incorporated in the lattice, neither as interstitial nor as substitutional species. Therefore, the decomposition  $\text{BH}_4^- \rightarrow \text{BH}_3 + \text{H}^-$  most likely takes place at the surface. The  $\text{H}^-$  ions remain in the lattice, locally converting  $\text{NaBH}_4$  into  $\text{NaH}$ . Both of these compounds have a similar rocksalt-like structure, so the ease with which  $\text{BH}_4^-$  ions can be substituted by  $\text{H}^-$  ions is not unexpected. The  $\text{H}^-$  ion is smaller than the  $\text{BH}_4^-$  ion, however, as reflected by the lattice constants 6.2 and 4.9 Å of  $\text{NaBH}_4$  and  $\text{NaH}$ , respectively. Substitution in  $\text{NaBH}_4$  of larger amounts of  $\text{BH}_4^-$  by  $\text{H}^-$  might lead to stress-induced cracking. This would enlarge the effective surface area, which promotes the decomposition reaction.

This scenario is consistent with the propositions extracted from optical and Raman spectroscopy that such anion substitutions lie at the origin of color centers in borohydrides and of the hydrogen–deuterium exchange in these systems.<sup>28</sup> Under conditions corresponding to eq 2, substitution of  $\text{BH}_4^-$  by  $\text{H}^-$  ions is calculated to happen easily in the dilute limit. This would be consistent with the observation of a mixed  $\text{NaBH}_4/\text{NaH}$  phase in the corresponding hydrogenation reaction.<sup>14</sup>

The  $\text{BH}_3$  molecules originating from the decomposition can escape to the gas phase and form  $\text{B}_2\text{H}_6$  (diborane) molecules, for instance. Alternatively, they may decompose immediately to form hydrogen and B. The presence of Mg and its subsequent conversion into  $\text{MgB}_2$  presents a stronger driving force for the formation of  $\text{BH}_4^-$  vacancies in  $\text{NaBH}_4$  and the substitution of  $\text{BH}_4^-$  by  $\text{H}^-$ , which boosts the decomposition scenario just sketched. The formation of H divacancies ( $\text{B}_2\text{H}_6^{2-}$  ions) in the lattice obstructs mass transport of B-related species, as divacancies are immobile. In the presence of  $\text{Mg}/\text{MgB}_2$ , these divacancies are relatively less important, however.

## ■ ASSOCIATED CONTENT

**S Supporting Information.** The raw data used to calculate the defect formation energies and the procedure for (re)calculating these under different thermodynamic conditions. This material is available free of charge via the Internet at <http://pubs.acs.org>.

## ■ AUTHOR INFORMATION

### Corresponding Author

\*E-mail: [g.brocks@tnw.utwente.nl](mailto:g.brocks@tnw.utwente.nl).

## ■ ACKNOWLEDGMENT

The work of D.C. has been financed by the European MC-RTN project “Complex Solid State Reactions for Energy Efficient Hydrogen Storage (COSY)”, contract no. 035366. We thank all our partners in this project for stimulating discussions. The work of G.A.W. is part of the research program of the “Stichting voor Fundamenteel Onderzoek der Materie (FOM)”. The use of supercomputer facilities was sponsored by the “Stichting Nationale Computerfaciliteiten (NCF)”. The latter two organizations are financially supported by the “Nederlandse Organisatie voor Wetenschappelijk Onderzoek (NWO)”.

## ■ REFERENCES

- (1) Züttel, A.; Borgschulte, A.; Orimo, S.-I. *Scr. Mater.* **2007**, *56*, 823–828.
- (2) Orimo, S.-I.; Nakamori, Y.; Eliseo, J. R.; Züttel, A.; Jensen, C. M. *Chem. Rev.* **2007**, *107*, 4111–4132.
- (3) Nakamori, Y.; Miwa, K.; Ninomiya, A.; Li, H.; Ohba, N.; Towata, S.; Züttel, A.; Orimo, S. *Phys. Rev. B* **2006**, *74*, 045126.
- (4) Alapati, S. V.; Johnson, J. K.; Sholl, D. S. *J. Phys. Chem. C* **2007**, *111*, 1584–1591.
- (5) Wolverton, C.; Siegel, D. J.; Akbarzadeh, A. R.; Ozoliņš, V. *J. Phys.: Condens. Matter* **2008**, *20*, 064228.
- (6) Ozoliņš, V.; Majzoub, E. H.; Wolverton, C. *J. Am. Chem. Soc.* **2009**, *131*, 230–237.
- (7) Vajo, J. J.; Olson, G. L. *Scr. Mater.* **2007**, *56*, 829–834.
- (8) Barkhordarian, G.; Klassen, T.; Dornheim, M.; Bormann, R. *J. Alloys Compd.* **2007**, *440*, L18–L21.

- (9) Urgnani, J.; Torres, F.; Palumbo, M.; Baricco, M. *Int. J. Hydrogen Energy* **2008**, *33*, 3111–3115.
- (10) Martelli, P.; Caputo, R.; Remhof, A.; Mauron, P.; Borgschulte, A.; Züttel, A. *J. Phys. Chem. C* **2010**, *114*, 7173–7177.
- (11) Caputo, R.; Garroni, S.; Olid, D.; Teixidor, F.; Suriñach, S.; Baró, M. D. *Phys. Chem. Chem. Phys.* **2010**, *12*, 15093–15100.
- (12) Garroni, S.; Pistidda, C.; Brunelli, M.; Vaughan, G.; Suriñach, S.; Baró, M. *Scr. Mater.* **2009**, *60*, 1129–1132.
- (13) Garroni, S.; Milanese, C.; Girella, A.; Marini, A.; Mulas, G.; Menéndez, E.; Pistidda, C.; Dornheim, M.; Suriñach, S.; Baró, M. *Int. J. Hydrogen Energy* **2010**, *35*, 5434–5441.
- (14) Pistidda, C.; Garroni, S.; Minella, C. B.; Dolci, F.; Jensen, T. R.; Nolis, P.; Bösenberg, U.; Cerenius, Y.; Lohstroh, W.; Fichtner, M.; Baró, M. D.; Bormann, R.; Dornheim, M. *J. Phys. Chem. C* **2010**, *114*, 21816–21823.
- (15) Hao, S.; Sholl, D. S. *Phys. Chem. Chem. Phys.* **2009**, *11*, 11106–11109.
- (16) van de Walle, C. G.; Neugebauer, J. *J. Appl. Phys.* **2004**, *95*, 3851–3879.
- (17) Wilson-Short, G. B.; Janotti, A.; Hoang, K.; Peles, A.; van de Walle, C. G. *Phys. Rev. B* **2009**, *80*, 224102.
- (18) van Setten, M. J.; de Wijs, G. A.; Brocks, G. *Phys. Rev. B* **2008**, *77*, 165115.
- (19) van Setten, M. J.; de Wijs, G. A.; Fichtner, M.; Brocks, G. *Chem. Mater.* **2008**, *20*, 4952–4956.
- (20) As Na has a low melting temperature of 371 K, it will be a liquid at the experimental temperatures of the current dehydrogenation reactions. Its heat of fusion is only 2.6 kJ/mol, however, implying that we can neglect this effect in the present calculations.
- (21) Chase, M. W. *J. Phys. Chem. Ref. Data Monogr.* **1998**, *9*, 1.
- (22) Ke, X.; Tanaka, I. *Phys. Rev. B* **2005**, *71*, 024117.
- (23) Kresse, G.; Hafner, J. *Phys. Rev. B* **1993**, *47*, R558.
- (24) Kresse, G.; Furthmüller, J. *Phys. Rev. B* **1996**, *54*, 11169.
- (25) Kresse, G.; Joubert, D. *Phys. Rev. B* **1999**, *59*, 1758.
- (26) Perdew, J. P.; Wang, Y. *Phys. Rev. B* **1991**, *45*, 13244.
- (27) Henkelman, G.; Uberuaga, B. P.; Jónsson, H. *J. Chem. Phys.* **2000**, *113*, 9901–9904.
- (28) Borgschulte, A.; Züttel, A.; Hug, P.; Racu, A.-M.; Schoenes, J. *J. Phys. Chem. A* **2008**, *112*, 4749–4753.
- (29) Borgschulte, A.; Gremaud, R.; Lodziana, Z.; Züttel, A. *Phys. Chem. Chem. Phys.* **2010**, *12*, 5061–5066.
- (30) van Setten, M. J.; de Wijs, G. A.; Popa, V. A.; Brocks, G. *Phys. Rev. B* **2005**, *72*, 073107.
- (31) van Setten, M. J.; de Wijs, G. A.; Brocks, G. *Phys. Rev. B* **2007**, *76*, 075125.
- (32) Babanova, O. A.; Solonin, A. V.; Stepanov, A. P.; Skripov, A. V.; Filinchuk, Y. *J. Phys. Chem. C* **2010**, *114*, 3712–3718.
- (33) Liang, C.; Liu, Y.; Jiang, Y.; Wei, Z.; Gao, M.; Pan, H.; Wang, Q. *Phys. Chem. Chem. Phys.* **2011**, *13*, 314–321.
- (34) In the eq 2 column of Table 2, the formation energy of  $\text{V}_{\text{BH}_3}^0$  is even negative, indicating that the  $\text{BH}_4^-/\text{H}^-$  substitution occurs spontaneously. This is a slight artifact of the chosen chemical potential for hydrogen. Lowering the temperature by 60 K would increase  $\mu_{\text{H}}$  sufficiently to remove this artifact.
- (35) Momma, K.; Izumi, F. *J. Appl. Crystallogr.* **2008**, *41*, 653.
- (36) Corey, R. L.; Shane, D. T.; Bowman, R. C., Jr.; Conradi, M. S. *J. Phys. Chem. C* **2008**, *112*, 18706–18710.
- (37) Shane, D. T.; Bowman, R. C., Jr.; Conradi, M. S. *J. Phys. Chem. C* **2009**, *113*, 5039–5042.